g-C_3N_4-based materials functionalized with Au, Ag and Au-Ag: an XPS study

Mattia Benedet,[1] Alberto Gasparotto,[1,2,a)] Gian Andrea Rizzi,[1,2] Davide Barreca,[2,a)] and Chiara Maccato[1,2]

[1] *Department of Chemical Sciences, Padova University and INSTM, 35131 Padova, Italy*

[2] *CNR-ICMATE and INSTM, Department of Chemical Sciences, Padova University, 35131 Padova, Italy*

(Received day Month year; accepted day Month year; published day Month year)

In the present contribution, X-ray photoelectron spectroscopy (XPS) was used to characterize the surface composition and elemental chemical states of graphitic carbon nitride (g-C_3N_4) materials decorated with highly dispersed noble metals (Au, Ag or Au+Ag). Samples were prepared through the electrophoretic deposition (EPD) of g-C_3N_4 on fluorine-doped tin oxide (FTO) substrates, and annealed at 500°C in Ar. The resulting systems were subsequently functionalized by radio frequency (RF)-sputtering, and finally annealed again under an Ar atmosphere. Material structural and morphological characterization revealed an intimate contact of the introduced noble metals with the underlying g-C_3N_4 matrix. Survey spectra, as well as detailed scans for the C 1s, N 1s, O 1s, Au 4f, Ag 3d and Sn 3d regions are presented and critically discussed. The obtained results evidence the presence of highly defective carbon nitride matrices functionalized either by low-sized Au nanoaggregates, atomically dispersed Ag, or partially alloyed Au-Ag core/shell nanoparticles.

Keywords: g-C_3N_4; Au; Ag; Au-Ag; electrophoresis; RF-sputtering; X-ray photoelectron spectroscopy

Acccession#: 01799, 01800, and 01801

Technique: XPS

Host Material: g-C_3N_4-Au; g-C_3N_4-Ag; g-C_3N_4-Au-Ag

Instrument: Perkin-Elmer Physical Electronics, Inc. 5600ci

Major Elements in Spectra: C, N, O, Au, Ag, Sn

Minor Elements in Spectra: none

Published Spectra: 19

Spectra in Electronic Record: 19

Spectral Category: comparison

INTRODUCTION

Over the last decade, graphitic carbon nitride (g-C_3N_4) has been thoroughly investigated as (photo)electrocatalyst for energy and environmental applications due to its favorable functional properties, chemical and thermal stability, low cost and non-toxicity (Refs. 1-4). For the above end-uses, the active material should be endowed with high active area and tailored surface defectivity and should be immobilized over a conductive support, to obtain good electrochemical performances and stability under operating conditions (Ref. 5). Among the various fabrication routes, the electrophoretic deposition (EPD) of g-C_3N_4 powders with *ad-hoc* properties represents a valuable option due to its simplicity and flexibility, even in the processing of nanoscale materials (Refs. 6-8). To further tune the system behavior, the obtained graphitic deposits can be decorated with highly dispersed noble metals (Au, Ag, Pt…), thus yielding functionalized g-C_3N_4-based architectures benefiting from chemical and electronic interfacial phenomena (Refs. 9-13).

Within this scenario, the present contribution reports on the EPD preparation of carbon nitride deposits on fluorine-doped tin oxide (FTO) substrates and the subsequent system modification with gold, silver and gold+silver. Whereas g-C_3N_4 was prepared in an exfoliated nanosized form starting from a melamine+cyanuric acid complex (Refs. 14, 15), Au and/or Ag were introduced by RF-sputtering, taking advantage on the infiltration power of this technique to achieve an effective intermixing between the various system components (Refs. 16).

A detailed XPS characterization, complemented by other analytical techniques, revealed that, regardless of the specific sample, the g-C_3N_4 matrix was highly defective and contained an appreciable amount of uncondensed -NH_x (x = 1,2) groups on the edges of heptazinic rings, whose occurrence is expected to favorably influence the system catalytic activity (Ref. 17, 18). The presence of these groups, along with the g-C_3N_4 porous structure and RF-sputtering bombardment action, promoted an efficient noble metal dispersion. Interestingly, whereas the sample containing only gold was characterized by low-sized Au(0) nanoparticles, silver alone was present in a quasi-atomically spread and partially oxidized form, revealing a different wetting behavior and chemical reactivity for the two elements. Finally, the Au+Ag-containing sample was characterized by bimetallic nanoparticles consisting of an Au core surrounded by an Au+Ag alloyed shell. Overall, such results provide useful research hints for a fine tuning of material properties and the design of advanced catalytic platforms for energy and environmental applications.

In this context, the present contribution is dedicated to the XPS analysis of g-C_3N_4-Au, g-C_3N_4-Ag, and g-C_3N_4-Au-Ag nanoscale deposits on FTO substrates, performed at room temperature using a non-monochromatized Al Kα X-ray source. Attention was specifically devoted to the C 1s, N 1s, O 1s, Au 4f, Ag 3d and Sn 3d regions, and to the study of their spectral features as a function of preparation conditions.

SPECIMEN DESCRIPTION (ACCESSION # 01799)

Host Material: g-C_3N_4-Au

CAS Registry #: unknown

Host Material Characteristics: homogeneous; solid; polycrystalline; semiconductor; composite; Thin Film

Chemical Name: graphitic carbon nitride-gold

a) Authors to whom correspondence should be addressed. e-mail: alberto.gasparotto@unipd.it (A.G.); davide.barreca@unipd.it (D.B.).

Source: specimen prepared by EPD of g-C_3N_4 on FTO, followed by gold RF-sputtering and final annealing in Ar atmosphere at 500°C

Host Composition: C, N, Au, O, Sn

Form: Supported nanocomposite thin film

Structure: The system structure, investigated by FT-IR spectroscopy, evidenced in the range 1200-1700 cm^{-1} the typical vibrational modes of the extended C-N-C network of g-C_3N_4, together with an additional peak at 810 cm^{-1} due to out-of-plane bending of heptazinic rings (Refs. 19, 20). In addition, a broad band at 3000-3500 cm^{-1} was observed, indicating the presence of uncondensed -NH_x groups (x = 1, 2) (Refs. 17, 21). Scanning electron microscopy (SEM) and transmission electron microscopy (TEM) analyses highlighted that the g-C_3N_4 deposit (thickness ≈ 15 μm) was characterized by islands of 10-20 μm, that left uncovered some regions of the underlying FTO substrate and were uniformly decorated by highly dispersed Au nanoparticles (average size = 2.0 nm).

History & Significance: Synthesis of g-C_3N_4 was carried out according to Ref. 14, preparing separately two solutions of melamine (1.5 g, Sigma-Aldrich) and cyanuric acid (1.5 g, Sigma Aldrich) in deionized water (50 mL) under heating at 60°C. The cyanuric acid solution was then added dropwise to the melamine one, yielding a white suspension containing a cyanuric acid+melamine supramolecular complex. After heating for 1 h, the suspension was filtered and the solid washed with a 50:50 water:ethanol solution and then dried at 60°C. The resulting powder was grinded, dispersed in an ethanol/ethylene glycol mixture (45+15 ml) and hence stirred under heating at 90°C for 3h. The obtained solid was filtered, washed and dried again, and finally heated for 2 h at 500°C in Ar to obtain an exfoliated g-C_3N_4 form (Ref. 14). Fabrication of the supported material was carried out following a modification of a previously reported procedure (Ref. 6). In brief, 10 mg of g-C_3N_4 were dispersed in toluene (100 mL), sonicated for 3 h and then deposited on FTO substrates (Sigma-Aldrich) by EPD (potential difference = 200 V; Heinzinger PNCs 2000-60 pos power generator; deposition time = 16 h). After thermal treatment at 500°C in Ar for 2.5 h, functionalization of g-C_3N_4 was carried out by RF-sputtering (ν = 13.56 MHz) from an Ar plasma in a custom-built two-electrode reactor (Ref. 22). Specifically, an Au metal target (BALTEC AG, 99.99%) was fixed on the RF electrode, whereas the FTO-supported g-C_3N_4 sample was mounted on the grounded one. Depositions were performed using the following settings: Ar flow rate = 10 standard cubic centimeters per minute (sccm); total pressure = 0.38 mbar; growth temperature = 60°C; RF-power = 5 W; process duration = 10 min. The resulting samples were ultimately annealed in Ar (500°C; 2.5 h).

As Received Condition: as grown

Analyzed Region: same as host material

Ex Situ Preparation/Mounting: Sample fixed with a metallic clip on a grounded sample holder and introduced into the analysis chamber through a fast entry lock system.

In Situ Preparation: none

Charge Control: No flood gun was used during analysis.

Temp. During Analysis: 298 K

Pressure During Analysis: $<10^{-8}$ Pa

Pre-analysis Beam Exposure: 180 s.

SPECIMEN DESCRIPTION (ACCESSION # 01800)

Host Material: g-C_3N_4-Ag

CAS Registry #: unknown

Host Material Characteristics: homogeneous; solid; polycrystalline; semiconductor; composite; Thin Film

Chemical Name: graphitic carbon nitride-silver

Source: specimen prepared by EPD of g-C_3N_4 on FTO, followed by silver RF-sputtering and final annealing in Ar atmosphere at 500°C

Host Composition: C, N, Ag, O, Sn

Form: Supported nanocomposite thin film

Structure: FT-IR, SEM and TEM analyses revealed that the g-C_3N_4 deposit had the same structural/morphological features reported for specimen g-C_3N_4-Au (see the previous accession). The average deposit thickness was ≈ 15 μm. However, as far as silver presence is concerned, no Ag nanoparticles could be clearly observed. Conversely, the use of high resolution-TEM in combination with energy-dispersive X-ray spectroscopy (EDXS) suggested the occurrence of silver in a quasi-atomically spread form.

History & Significance: The synthesis and deposition procedure for g-C_3N_4 was the same reported for specimen g-C_3N_4-Au (see the previous accession). Similarly, g-C_3N_4 functionalization with Ag was carried out by RF-sputtering in the same reactor described above under the following conditions: Ag metal target (BALTEC AG, 99.9%); Ar flow rate = 10 sccm; total pressure = 0.38 mbar; growth temperature = 60°C; RF-power = 5 W; process duration = 20 min.

As Received Condition: as grown

Analyzed Region: same as host material

Ex Situ Preparation/Mounting: Sample fixed with a metallic clip on a grounded sample holder and introduced into the analysis chamber through a fast entry lock system.

In Situ Preparation: none

Charge Control: No flood gun was used during analysis.

Temp. During Analysis: 298 K

Pressure During Analysis: $<10^{-8}$ Pa

Pre-analysis Beam Exposure: 180 s.

SPECIMEN DESCRIPTION (ACCESSION # 01801)

Host Material: g-C_3N_4-Au-Ag

CAS Registry #: unknown

Host Material Characteristics: homogeneous; solid; polycrystalline; semiconductor; composite; Thin Film

Chemical Name: graphitic carbon nitride-gold-silver

Source: specimen prepared by EPD of g-C_3N_4 on FTO, followed by sequential RF-sputtering of gold and silver, and final annealing in Ar atmosphere at 500°C

Host Composition: C, N, Au, Ag, O, Sn

Form: Supported nanocomposite thin film

Structure: Sample characterization by FT-IR, SEM and TEM indicated that the g-C_3N_4 deposit had structural and

morphological characteristics analogous to those of the former two samples (see previous accessions). The mean deposit thickness was ≈ 15 μm. The use of high resolution-TEM and EDXS revealed that the sequential sputtering of Au and Ag yielded the formation of bimetallic nanoparticles consisting of an Au core and an alloyed Au+Ag shell. The average size of such NPs was 3.0 nm, slightly bigger than in the case of specimen g-C_3N_4-Au.

History & Significance: The synthesis and deposition procedure for g-C_3N_4 is the same reported for the two previous specimens. Subsequently, g-C_3N_4 was functionalized with Au and Ag by sequential RF-sputtering of gold and silver using the same deposition conditions reported in accessions # 01799 and # 01800, respectively.

As Received Condition: as grown

Analyzed Region: same as host material

Ex Situ Preparation/Mounting: Sample fixed with a metallic clip on a grounded sample holder and introduced into the analysis chamber through a fast entry lock system.

In Situ Preparation: none

Charge Control: No flood gun was used during analysis.

Temp. During Analysis: 298 K

Pressure During Analysis: $<10^{-8}$ Pa

Pre-analysis Beam Exposure: 180 s.

INSTRUMENT DESCRIPTION

Manufacturer and Model: Perkin-Elmer Physical Electronics, Inc. 5600ci

Analyzer Type: spherical sector

Detector: Channeltron

Number of Detector Elements: 16

INSTRUMENT PARAMETERS COMMON TO ALL SPECTRA

■*Spectrometer*

Analyzer Mode: constant pass energy

Throughput ($T=E^N$): N=0

Excitation Source Window: 1.5 micron Al window

Excitation Source: Al Ka

Source Energy: 1486.6 eV

Source Strength: 200 W

Source Beam Size: > 25000 μm x > 25000 μm

Signal Mode: multichannel direct

■*Geometry*

Incident Angle: 9˚

Source-to-Analyzer Angle: 53.8˚

Emission Angle: 45˚

Specimen Azimuthal Angle: 0˚

Acceptance Angle from Analyzer Axis: 0˚

Analyzer Angular Acceptance Width: 14˚ × 14˚

■*Ion Gun*

Manufacturer and Model: PHI 04-303 A

Energy: 3000 eV

Current: 0.4 mA/cm2

Current Measurement Method: Faraday cup

Sputtering Species: Ar^+

Spot Size (unrastered): 250 μm

Raster Size: 2000 μm x 2000 μm

Incident Angle: 40 ˚

Polar Angle: 45 ˚

Azimuthal Angle: 111 ˚

Comment: differentially pumped ion gun

DATA ANALYSIS METHOD

Energy Scale Correction: None

Recommended Energy Scale Shift: 0 eV for all specimens

Peak Shape and Background Method: After performing a Shirley-type background subtraction (Ref. 23), BE and full width at half maximum (FWHM) values were determined by least-squares fitting adopting Gaussian/Lorentzian functions.

Quantitation Method: Atomic concentrations were calculated by peak area integration, using sensitivity factors provided by PHI V5.4A software.

ACKNOWLEDGMENTS

The National Council of Research (Progetti di Ricerca @CNR - avviso 2020 - ASSIST), Padova University (DOR 2020-2022, P-DiSC#04BIRD2020-UNIPD EUREKA), AMGA Foundation (NYMPHEA project) and INSTM Consortium (INSTM21PDBARMAC– ATENA, INSTM21PDGASPAROTTO - NANO^{MAT}) are acknowledged for financial support. Thanks are also due to Dr. Lorenzo Bigiani and Dr. Leonardo Girardi for their valuable experimental support.

CONFLICT OF INTEREST

The authors have no conflicts to disclose.

DATA AVAILABILITY

The data that support the findings of this study are available within the article and its supplementary material.

REFERENCES

1. S. Cao, J. Low, J. Yu, and M. Jaroniec, Adv. Mater. **27**, 2150 (2015).
2. M. Jourshabani, B.-K. Lee, and Z. Shariatinia, Appl. Catal., B **276**, 119157 (2020).
3. G. Liao, Y. Gong, L. Zhang, H. Gao, G.-J. Yang, and B. Fang, Energy Environ. Sci. **12**, 2080 (2019).
4. S. Ye, L.-G. Qiu, Y.-P. Yuan, Y.-J. Zhu, J. Xia, and J.-F. Zhu, J. Mater. Chem. A **1**, 3008 (2013).
5. W. K. Darkwah, and Y. Ao, Nanoscale Res. Lett. **13**, 388 (2018).
6. J. Xu, and M. Shalom, ACS Appl. Mater. Interfaces **8**, 13058 (2016).
7. R. Malik, and V. K. Tomer, Renew. Sust. Energ. Rev. **135**, 110235 (2021).

8. M. Z. Rahman, and C. B. Mullins, Acc. Chem. Res. **52**, 248 (2019).
9. A. Nasri, B. Jaleh, Z. Nezafat, M. Nasrollahzadeh, S. Azizian, H. W. Jang, and M. Shokouhimehr, Ceram. Int. **47**, 3565 (2021).
10. J. Qin, J. Huo, P. Zhang, J. Zeng, T. Wang, and H. Zeng, Nanoscale **8**, 2249 (2016).
11. R. Liu, W. Yang, G. He, W. Zheng, M. Li, W. Tao, and M. Tian, ACS Omega **5**, 19615 (2020).
12. M. A. Gondal, A. A. Adeseda, S. G. Rashid, A. Hameed, M. Aslam, I. M. I. Ismail, U. Baig, M. A. Dastageer, A. R. Al-Arfaj, and A. U. Rehman, J. Mol. Catal. A: Chem. **423**, 114 (2016).
13. A. Sudhaik, P. Raizada, P. Shandilya, D.-Y. Jeong, J.-H. Lim, and P. Singh, J. Ind. Eng. Chem. **67**, 28 (2018).
14. W. Liu, Z. Zhang, D. Zhang, R. Wang, Z. Zhang, and S. Qiu, RSC Adv. **10**, 28848 (2020).
15. M. Shalom, S. Inal, C. Fettkenhauer, D. Neher, and M. Antonietti, J. Am. Chem. Soc. **135**, 7118 (2013).
16. L. Armelao, D. Barreca, G. Bottaro, A. Gasparotto, C. Maccato, E. Tondello, O. I. Lebedev, S. Turner, G. Van Tendeloo, C. Sada, and U. L. Štangar, ChemPhysChem **10**, 3249 (2009).
17. Y. Xiao, G. Tian, W. Li, Y. Xie, B. Jiang, C. Tian, D. Zhao, and H. Fu, J. Am. Chem. Soc. **141**, 2508 (2019).
18. M. Majdoub, Z. Anfar, and A. Amedlous, ACS Nano **14**, 12390 (2020).
19. K. Wang, Q. Li, B. Liu, B. Cheng, W. Ho, and J. Yu, Appl. Catal., B **176-177**, 44 (2015).
20. X. Yuan, K. Luo, K. Zhang, J. He, Y. Zhao, and D. Yu, J. Phys. Chem. A **120**, 7427 (2016).
21. T. S. Miller, A. B. Jorge, T. M. Suter, A. Sella, F. Corà, and P. F. McMillan, Phys. Chem. Chem. Phys. **19**, 15613 (2017).
22. D. Barreca, A. Gasparotto, E. Tondello, G. Bruno, and M. Losurdo, J. Appl. Phys. **96**, 1655 (2004).
23. D. A. Shirley, Phys. Rev. B **5**, 4709 (1972).
24. J. Wang, and W.-D. Zhang, Electrochim. Acta **71**, 10 (2012).
25. L. Liang, L. Shi, F. Wang, H. Wang, and W. Qi, Sustain. Energy Fuels **4**, 5179 (2020).
26. H. Yu, R. Shi, Y. Zhao, T. Bian, Y. Zhao, C. Zhou, G. I. N. Waterhouse, L.-Z. Wu, C.-H. Tung, and T. Zhang, Adv. Mater. **29**, 1605148 (2017).
27. J. Fu, B. Zhu, C. Jiang, B. Cheng, W. You, and J. Yu, Small **13**, 1603938 (2017).
28. Q. Zhu, B. Qiu, M. Du, J. Ji, M. Nasir, M. Xing, and J. Zhang, ACS Sustain. Chem. Eng. **8**, 7497 (2020).
29. Q. Liang, Z. Li, Z.-H. Huang, F. Kang, and Q.-H. Yang, Adv. Funct. Mater. **25**, 6885 (2015).
30. X. Chen, Y. Liu, X.-X. Ke, R. Weerasooriya, H. Li, L.-C. Wang, and Y.-C. Wu, J. Alloys Compd. **853**, 157365 (2021).
31. J. F. Moulder, W. F. Stickle, P. E. Sobol, and K. D. Bomben, *Handbook of X-ray Photoelectron Spectroscopy* (Perkin Elmer Corporation, Eden Prairie, MN, USA, 1992).
32. http://srdata.nist.gov/xps.
33. A. Ahmed, A. Hayat, M. H. Nawaz, P. John, and M. Nasir, J. Colloid Interf. Sci. **558**, 230 (2020).
34. D. Briggs, and M. P. Seah, *Practical Surface Analysis: Auger and X-ray Photoelectron Spectroscopy* (2nd ed., Wiley, New York, 1990).
35. D. Barreca, A. Gasparotto, C. Maragno, E. Tondello, and S. Gialanella, J. Nanosci. Nanotechnol. **7**, 2480 (2007).
36. D. Barreca, A. Bovo, A. Gasparotto, and E. Tondello, Surf. Sci. Spectra **10**, 21 (2003).
37. S. Peters, S. Peredkov, M. Neeb, W. Eberhardt, and M. Al-Hada, Surf. Sci. **608**, 129 (2013).
38. D. Barreca, A. Gasparotto, C. Maragno, and E. Tondello, Surf. Sci. Spectra **13**, 1 (2006).
39. T. E. G. Alivio, N. A. Fleer, J. Singh, G. Nadadur, M. Feng, S. Banerjee, and V. K. Sharma, Environ. Sci. Technol. **52**, 7269 (2018).
40. T. Zhang, H. Xu, S. Xu, B. Dong, Z. Wu, X. Zhang, L. Zhang, and H. Song, RSC Adv. **6**, 51609 (2016).
41. S. Nishimura, A. T. N. Dao, D. Mott, K. Ebitani, and S. Maenosono, J. Phys. Chem. C **116**, 4511 (2012).
42. M. S. Nasir, G. Yang, I. Ayub, S. Wang, and W. Yan, Appl. Catal., B **270**, 118900 (2020).

SPECTRAL FEATURES TABLE							
Spectrum ID #	**Element/ Transition**	**Peak Energy (eV)**	**Peak Width FWHM (eV)**	**Peak Area (eV x cts/s)**	**Sensitivity Factor**	**Concentration (at. %)**	**Peak Assignment**
01799-02[a]	C 1s	284.8	2.1	489.8	0.296	2.7	Adventitious surface contamination
01799-02[a]	C 1s	286.2	2.2	1283.0	0.296	7.2	C-NH_x (x=1,2) species on the edges of heptazinic rings
01799-02[a]	C 1s	288.2	2.1	5125.2	0.296	28.6	N-C=N carbon atoms in the g-C_3N_4 aromatic rings
01799-03[b]	N 1s	398.6	2.1	8292.5	0.477	28.7	Two-coordinated C=N-C nitrogen atoms in g-C_3N_4
01799-03[b]	N 1s	399.9	2.0	3717.3	0.477	12.9	Tertiary N-$(C)_3$ nitrogen atoms in g-C_3N_4
01799-03[b]	N 1s	401.1	2.2	2001.7	0.477	6.9	NH_x (x=1,2) uncondensed amino groups
01799-03[b]	N 1s	404.2	3.4	1038.5	0.477	3.7	Excitation of π-electrons in heptazine rings
01799-04[c]	O 1s	530.4	1.8	1925.3	0.711	4.5	Lattice oxygen from the FTO substrate
01799-04[c]	O 1s	531.9	3.1	445.7	0.711	1.0	–OH groups adsorbed on g-C_3N_4 anionic vacancies
01799-05[d]	Au 4f	…	…	7332.0	6.25	1.9	Au(0) nanoparticles
01799-05	Au $4f_{7/2}$	84.2	1.8	…	…	…	Au(0) nanoparticles
01799-05	Au $4f_{5/2}$	87.8	1.8	…	…	…	Au(0) nanoparticles
01799-06[e]	Sn 3d	...	…	…	…	1.9	Sn(IV) from FTO
01799-06	Sn $3d_{5/2}$	486.7	1.8	5522.0	4.725	…	Sn(IV) from FTO
01799-06	Sn $3d_{3/2}$	495.1	1.8	3681.0	…	…	Sn(IV) from FTO
01800-02[a]	C 1s	284.8	2.3	739.4	0.296	3.6	Adventitious surface contamination
01800-02[a]	C 1s	286.2	1.9	1347.8	0.296	6.5	C-NH_x (x=1,2) species on the edges of heptazinic rings
01800-02[a]	C 1s	288.2	2.2	5614.8	0.296	27.1	N-C=N carbon atoms in the g-C_3N_4 aromatic rings
01800-03[b]	N 1s	398.7	2.1	10407.0	0.477	31.2	Two-coordinated C=N-C nitrogen atoms in g-C_3N_4
01800-03[b]	N 1s	399.9	2.0	4465.4	0.477	13.4	Tertiary N-$(C)_3$ nitrogen atoms in g-C_3N_4
01800-03[b]	N 1s	401.1	2.2	2424.1	0.477	7.3	NH_x (x=1,2) uncondensed amino groups
01800-03[b]	N 1s	404.2	3.5	929.5	0.477	2.8	Excitation of π-electrons in heptazine rings
01800-04[c]	O 1s	530.4	1.8	1950.5	0.711	3.9	Lattice oxygen from the FTO substrate
01800-04[c]	O 1s	531.8	2.5	909.5	0.711	1.8	–OH groups adsorbed on g-C_3N_4 anionic vacancies
01800-05[f]	Ag 3d	…	…	1503.0	5.987	0.4	Atomically spread silver
01800-05	Ag $3d_{5/2}$	368.5	2.5	…	…	…	Atomically spread silver
01800-05	Ag $3d_{3/2}$	374.5	2.5	…	…	…	Atomically spread silver
01800-06[e]	Sn 3d	...	…	…	…	2.0	Sn(IV) from FTO
01800-06	Sn $3d_{5/2}$	486.7	1.8	6716.0	4.725	…	Sn(IV) from FTO
01800-06	Sn $3d_{3/2}$	495.2	1.8	4477.3	…	…	Sn(IV) from FTO
01801-02[a]	C 1s	284.8	2.1	654.5	0.296	3.5	Adventitious surface contamination
01801-02[a]	C 1s	286.2	2.2	1294.4	0.296	7.1	C-NH_x (x=1,2) species on the edges of heptazinic rings
01801-02[a]	C 1s	288.3	2.1	5323.1	0.296	28.8	N-C=N carbon atoms in the g-C_3N_4 aromatic rings
01801-03[b]	N 1s	398.7	1.9	8139.4	0.477	27.4	Two-coordinated C=N-C nitrogen atoms in g-C_3N_4
01801-03[b]	N 1s	399.9	2.0	3646.1	0.477	12.3	Tertiary N-$(C)_3$ nitrogen atoms in g-C_3N_4
01801-03[b]	N 1s	401.1	2.2	2390.4	0.477	8.0	NH_x (x=1,2) uncondensed amino groups

01801-03[b]	N 1s	404.2	3.5	953.1	0.477	3.2	Excitation of π-electrons in heptazine rings
01801-04[c]	O 1s	530.4	1.8	1574.9	0.711	3.6	Lattice oxygen from the FTO substrate
01801-04[c]	O 1s	531.8	2.5	1063.1	0.711	2.4	–OH groups adsorbed on g-C_3N_4 anionic vacancies
01801-05[d]	Au 4f	…	…	8933.0	6.25	2.3	Au in core/shell Au/Au+Ag nanoparticles
01801-05	Au $4f_{7/2}$	84.3	1.9	…	…	…	Au in core/shell Au/Au+Ag nanoparticles
01801-05	Au $4f_{5/2}$	87.9	1.9	…	…	…	Au in core/shell Au/Au+Ag nanoparticles
01801-06[f]	Ag 3d	…	…	2053.0	5.987	0.5	Ag in core/shell Au/Au+Ag nanoparticles
01801-06	Ag $3d_{5/2}$	368.3	2.0	…	…	…	Ag in core/shell Au/Au+Ag nanoparticles
01801-06	Ag $3d_{3/2}$	374.3	2.0	…	…	…	Ag in core/shell Au/Au+Ag nanoparticles
01801-07[e]	Sn 3d	...	…		…	0.9	Sn(IV) from FTO
01801-07	Sn $3d_{5/2}$	486.7	1.8	2698.0	4.725	…	Sn(IV) from FTO
01801-07	Sn $3d_{3/2}$	495.0	1.8	1798.7	…	…	Sn(IV) from FTO

[a] The sensitivity factor is referred to the whole C 1s signal.
[b] The sensitivity factor is referred to the whole N 1s signal.
[c] The sensitivity factor is referred to the whole O 1s signal.
[d] The peak area, sensitivity factor, and concentration are referred to the whole Au 4f signal.
[e] Tin atomic percentage was evaluated basing on the area and sensitivity factor for the $Sn3d_{5/2}$ component reported in the next line.
[f] The peak area, sensitivity factor, and concentration are referred to the whole Ag 3d signal.

Footnote to Spectra 01799-01, 01800-01 and 01801-01: Wide-scan spectra confirmed the functionalization of g-C_3N_4 with Au-, Ag- and Au-Ag-containing species, as well as Sn signals due to an incomplete FTO substrate coverage.

Footnote to Spectra 01799-02, 01800-02 and 01801-02: For all specimens, the C 1s peak could be deconvoluted into three components: (**I**) BE = 284.8 eV, due to adventitious carbon contamination (Refs. 24, 25); (**II**) BE = 286.2 eV, due to C-NH_x groups (x = 1, 2) on the edges of heptazine rings (the basic structural sub-units of g-C_3N_4) (Refs. 9, 26) and to a possible minor contribution even from -C≡N groups (Ref. 21); (**III**) the main one, BE = 288.2 eV, due N-C=N carbon atoms in the aromatic rings (Refs. 9, 10, 24, 27). Irrespective of the considered sample, the modest contribution of component (**I**) to the overall C 1s signal indicated a good system purity. The relative contribution of component (**II**) with respect to (**III**) suggested an appreciable material defectivity.

Footnote to Spectra 01799-03, 01800-03 and 01801-03: Four bands contributed to the N 1s signal. Component (**IV**), the most intense one (mean BE = 398.6 eV), originates from two-coordinated nitrogen atoms (C=N-C, N_{2c}) (Refs. 9, 28, 29) and from an eventual minor contribution from -C≡N groups (see above) (Refs. 26, 27). In a different way, component (**V**) (average BE = 399.9 eV) can be related to tertiary [N-$(C)_3$, N_{3c}] N atoms of the carbon nitride framework (Refs. 14, 21, 24, 26, 27, 29). Band (**VI**) (average BE = 401.1 eV) was indicative of terminal NH_x (x = 1, 2) moieties (Refs. 17, 21, 24-27). The presence of such species, that should not be present in an ideal, fully condensed g-C_3N_4 structure, is responsible for a mean N/C atomic ratio slightly higher than the value expected for stoichiometric C_3N_4. Finally, the minor band (**VII**) (mean BE = 404.2 eV) was ascribed to π-electrons excitations (Refs. 9, 14, 29, 30).

Footnote to Spectra 01799-04, 01800-04 and 01801-04: For all specimens, two bands contributed to the O 1s signal. The main one (**VIII**), centered at BE = 530.4 eV, was due to FTO lattice oxygen (Refs. 31, 32), and arose from an incomplete substrate coverage (see also Footnote to Spectra 01799-06, 01800-06 and 01801-07). A second component (**IX**) at 531.8 eV was attributed to -OH groups originating from the dissociative chemisorption of water on g-C_3N_4. (Refs. 27, 28). For accession # 01800, component (**VIII**) contains even a minor contribution from silver oxide (see also below) which, however, cannot be deconvoluted from FTO oxygens due to the very similar BE values (Refs. 31-33).

Footnote to Spectra 01799-05 and 01801-05: The Au 4f peak indicated that gold was present in a metallic state (Refs. 31, 32, 34, 35). More specifically, for both accessions # 01799 and # 01801, the Au $4f_{7/2}$ BE component was ≈0.3 eV higher than literature values reported not only for Au-C_3N_4 nanocomposites (Refs. 9, 30), but also for bulk gold (Refs. 31, 34). This phenomenon might be related to: i) the presence of core-level shifts, typically observed for low-sized gold nanostructures (Refs. 36, 37); ii) the occurrence of a partial Ag-Au alloying (Ref. 38). These conclusions are corroborated by the above discussed TEM results (see the 'Structure' subsection for the various specimens).

Footnote to Spectra 01800-05 and 01801-06: Analysis of the Ag 3d signal indicated a possible partial contribution of oxidized Ag(I) species for accession # 01800 (Refs. 10, 33, 39), as reported in the case of nanocomposites containing monometallic silver nanoparticles (Ref. 16). Conversely, as far as accession # 01801 is concerned, although a detailed estimation of the Ag(I)/Ag(0) mutual contents is prevented by their very close energy position, silver was present in an essentially metallic state (Refs. 11, 31, 32). In fact, upon going from accession # 01800 to accession # 01801, the Ag $3d_{5/2}$ signal shifted from BE = 368.5 eV to 368.3 eV. The occurrence of a similar Ag 3d BE red-shift, previously documented for liquid phase-prepared Au-Ag alloyed nanocrystals (Refs. 39, 40) and Au(core)-Ag(shell) nanoparticles (Ref. 41), could be traced back to a gold→silver electron transfer (Refs. 39, 41). This phenomenon, accompanied by a simultaneous Au-Ag alloying, has been reported to inhibit Ag oxidation. This conclusion was further corroborated by the fact that the full width at half maximum (FWHM) of the Ag 3d components became narrower (from 2.5 eV to 2.0 eV) upon going from accession # 01800 to accession # 01801.

Footnote to Spectra 01799-06, 01800-06 and 01801-07: The Sn 3d peak position [BE(Sn $3d_{5/2}$) = 486.7 eV, spin-orbit splitting (SOS) ≈ 8.4 eV] was in agreement with literature data for Sn(IV) (Refs. 31, 34, 42). The detection of Sn signals from FTO was related to the island-like morphology of discontinuous g-C_3N_4 deposits, resulting in an incomplete substrate coverage (see SEM images reported as insets in figure accessions # 01799-01, 01800-01, and 01801-01).

ANALYZER CALIBRATION TABLE							
Spectrum ID #	**Element/ Transition**	**Peak Energy (eV)**	**Peak Width FWHM (eV)**	**Peak Area (eV x cts/s)**	**Sensitivity Factor**	**Concentration (at. %)**	**Peak Assignment**
…[a]	Au $4f_{7/2}$	84.0	1.4	186403	...	...	Au(0)
…[a]	Cu $2p_{3/2}$	932.7	1.6	86973	...	...	Cu(0)

[a] The peak was acquired after Ar^+ erosion.

GUIDE TO FIGURES					
Spectrum (Accession) #	**Spectral Region**	**Voltage Shift***	**Multiplier**	**Baseline**	**Comment #**
01799-01	Survey	0	1	0	…
01799-02	C 1s	0	1	0	…
01799-03	N 1s	0	1	0	…
01799-04	O 1s	0	1	0	…
01799-05	Au 4f	0	1	0	…
01799-06	Sn 3d	0	1	0	…
01800-01	Survey	0	1	0	…
01800-02	C 1s	0	1	0	…
01800-03	N 1s	0	1	0	…
01800-04	O 1s	0	1	0	…
01800-05	Ag 3d	0	1	0	…
01800-06	Sn 3d	0	1	0	…
01801-01	Survey	0	1	0	…
01801-02	C 1s	0	1	0	…
01801-03	N 1s	0	1	0	…
01801-04	O 1s	0	1	0	…
01801-05	Au 4f	0	1	0	…
01801-06	Ag 3d	0	1	0	…
01801-07	Sn 3d	0	1	0	…

* Voltage shift of the archived (as measured) spectrum relative to the printed figure. The figure reflects the recommended energy scale correction due to a calibration correction, sample charging, flood gun, or other phenomena.

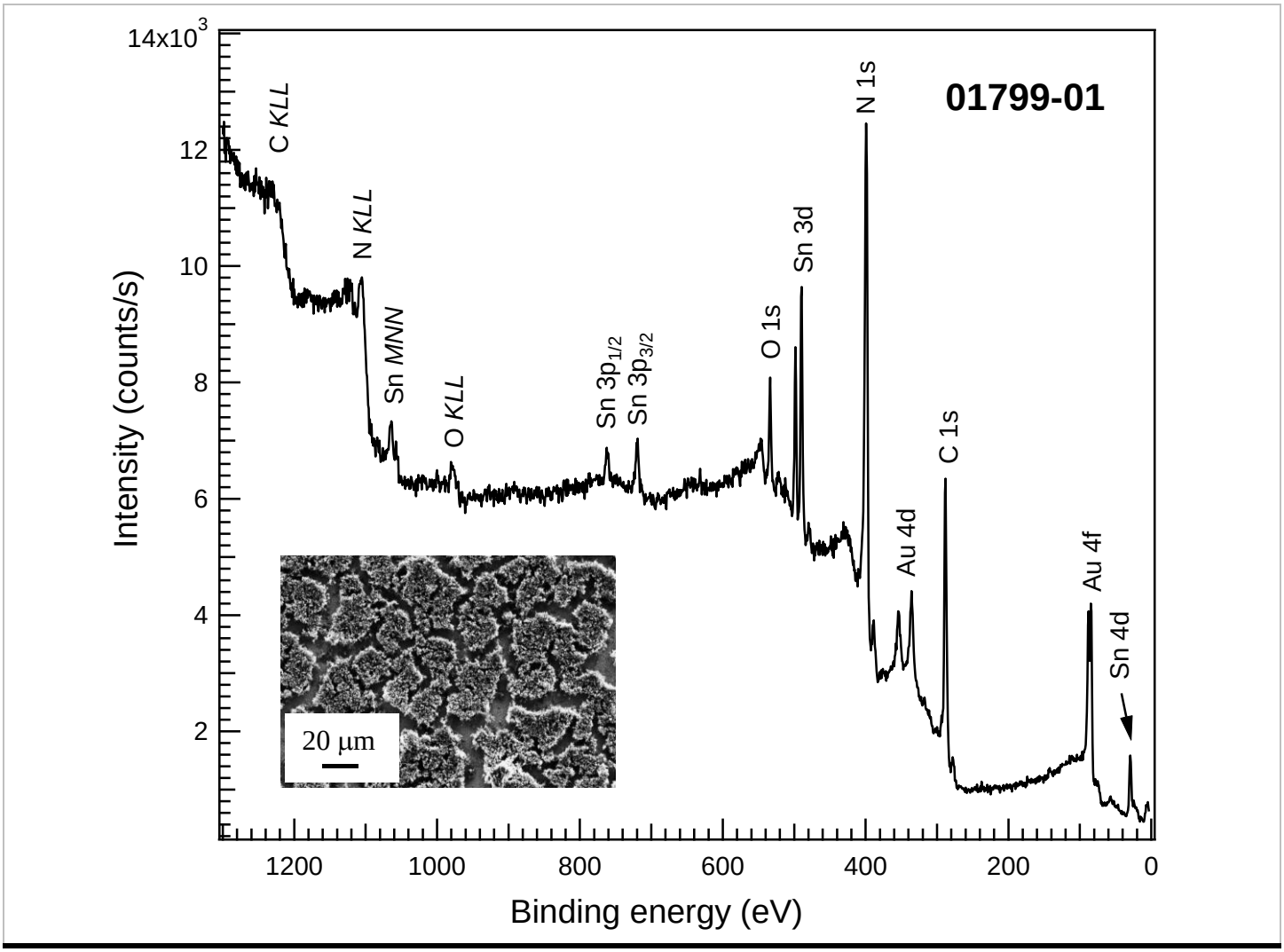

Publish in *Surface Science Spectra*: Yes ☒ No ☐

Accession #	01799-01
Host Material	C_3N_4-Au
Technique	XPS
Spectral Region	survey
Instrument	Perkin-Elmer Physical Electronics, Inc. 5600ci
Excitation Source	Al Ka
Source Energy	1486.6 eV
Source Strength	200 W
Source Size	>25 mm x >25 mm
Analyzer Type	spherical sector analyzer
Incident Angle	9 ˚
Emission Angle	45 ˚
Analyzer Pass Energy	187.85 eV
Analyzer Resolution	1.9 eV
Total Signal Accumulation Time	1300.8 s
Total Elapsed Time	1430.9 s
Number of Scans	40
Effective Detector Width	1.9 eV

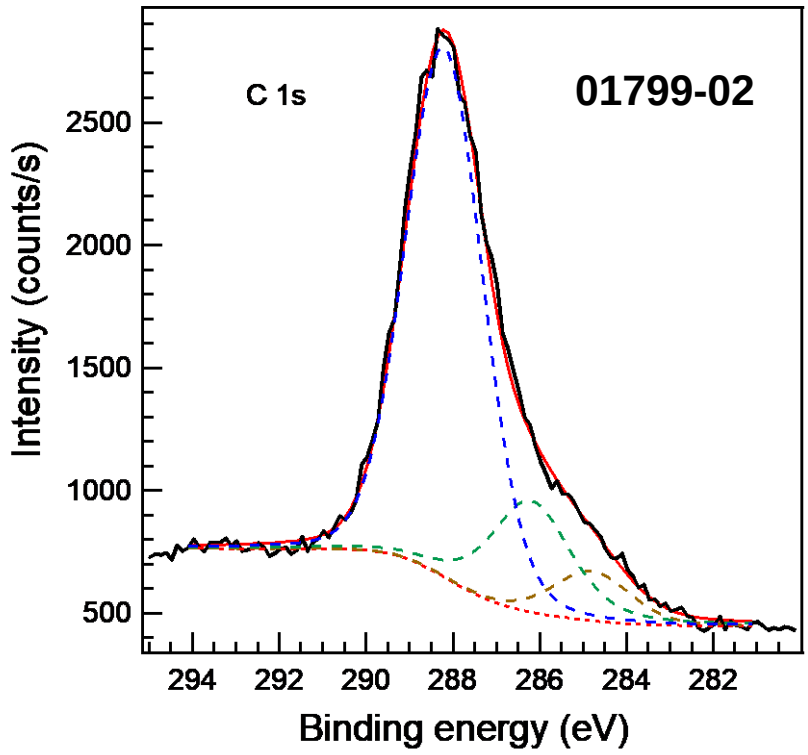

Publish in *SSS*: Yes X No ☐

- **Accession #: 01799-02**
- **Host Material:** C_3N_4-Au
- **Technique:** XPS
- **Spectral Region:** C 1s

Instrument: Perkin-Elmer Physical Electronics, Inc. 5600ci
Excitation Source: Al Ka
Source Energy: 1486.6 eV
Source Strength: 200 W
Source Size: >25 mm x >25 mm
Analyzer Type: spherical sector
Incident Angle: 9 °
Emission Angle: 45 °
Analyzer Pass Energy 58.7 eV
Analyzer Resolution: 0.6 eV
Total Signal Accumulation Time: 205.5 s
Total Elapsed Time: 226.1 s

Number of Scans: 30

Effective Detector Width: 0.6 eV

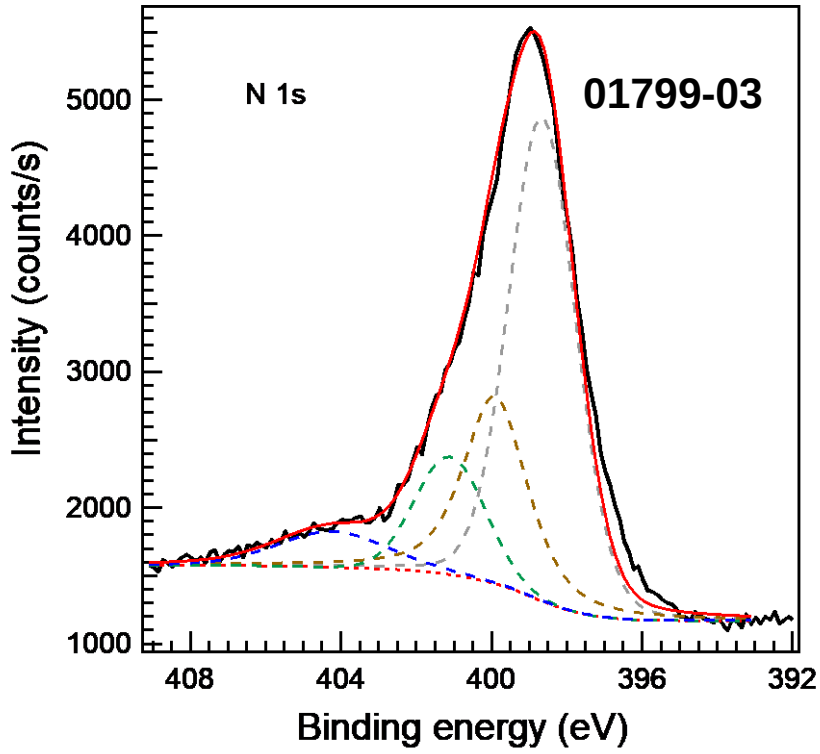

Publish in *SSS*: Yes X No ☐

- **Accession #: 01799-03**
- **Host Material:** C_3N_4-Au
- **Technique:** XPS
- **Spectral Region:** N 1s

Instrument: Perkin-Elmer Physical Electronics, Inc. 5600ci
Excitation Source: Al Ka
Source Energy: 1486.6 eV
Source Strength: 200 W
Source Size: >25 mm x >25 mm
Analyzer Type: spherical sector
Incident Angle: 9 °
Emission Angle: 45 °
Analyzer Pass Energy 58.7 eV
Analyzer Resolution: 0.6 eV
Total Signal Accumulation Time: 241.5 s
Total Elapsed Time: 265.7 s

Number of Scans: 30

Effective Detector Width: 0.6 eV

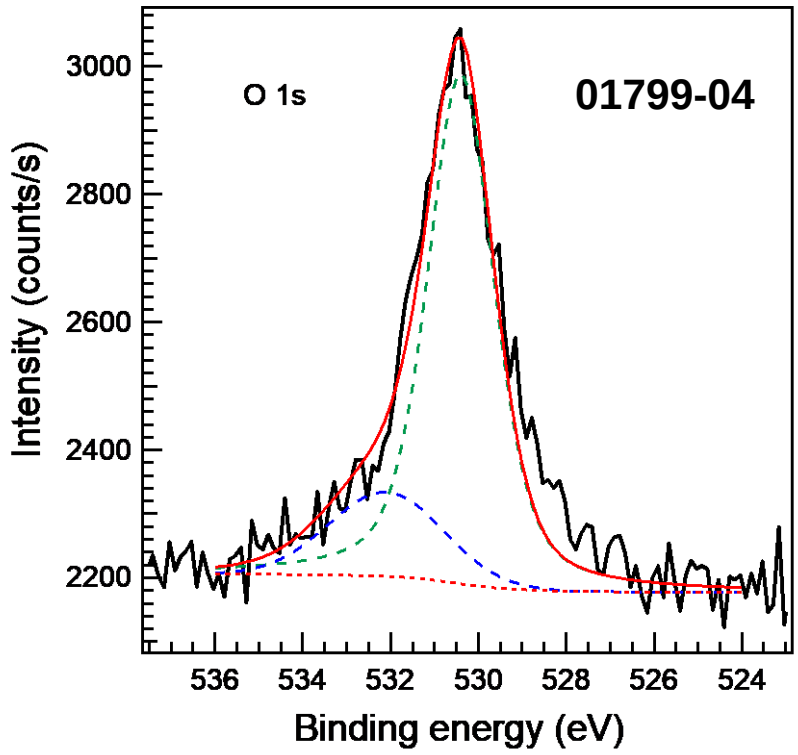

Publish in *SSS*: Yes X No ☐

- **Accession #: 01799-04**
- **Host Material:** C_3N_4-Au
- **Technique:** XPS
- **Spectral Region:** O 1s

Instrument: Perkin-Elmer Physical Electronics, Inc. 5600ci
Excitation Source: Al Ka
Source Energy: 1486.6 eV
Source Strength: 200 W
Source Size: >25 mm x >25 mm
Analyzer Type: spherical sector
Incident Angle: 9 °
Emission Angle: 45 °
Analyzer Pass Energy 58.7 eV
Analyzer Resolution: 0.6 eV
Total Signal Accumulation Time: 322.0 s
Total Elapsed Time: 354.2 s

Number of Scans: 40

Effective Detector Width: 0.6 eV

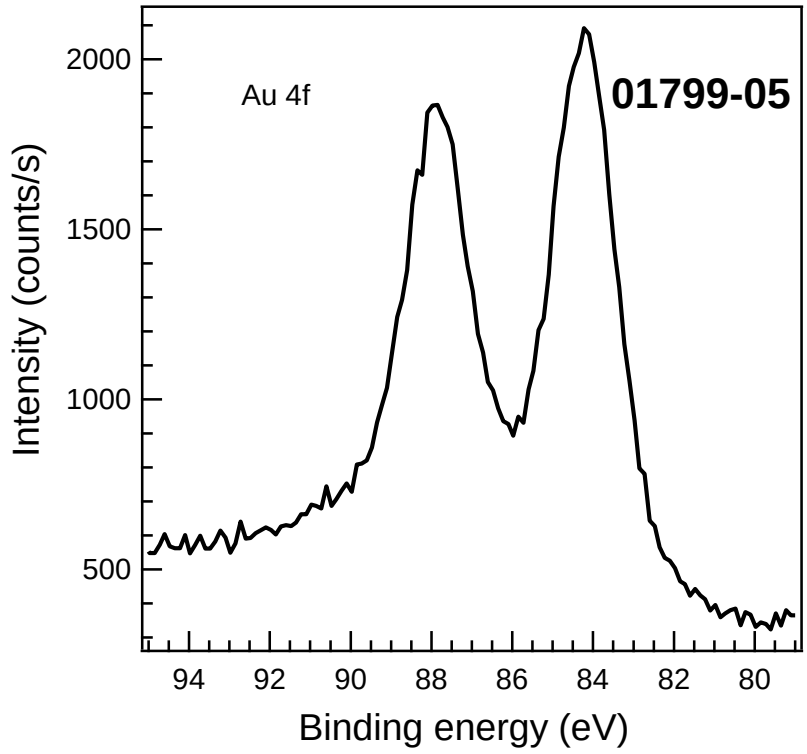

Publish in *SSS*: Yes X No ☐

- **Accession #: 01799-05**
- **Host Material:** C_3N_4-Au
- **Technique:** XPS
- **Spectral Region:** Au 4f

Instrument: Perkin-Elmer Physical Electronics, Inc. 5600ci
Excitation Source: Al Ka
Source Energy: 1486.6 eV
Source Strength: 200 W
Source Size: >25 mm x >25 mm
Analyzer Type: spherical sector
Incident Angle: 9 °
Emission Angle: 45 °
Analyzer Pass Energy 58.7 eV
Analyzer Resolution: 0.6 eV
Total Signal Accumulation Time: 322.0 s
Total Elapsed Time: 354.2 s

Number of Scans: 40

Effective Detector Width: 0.6 eV

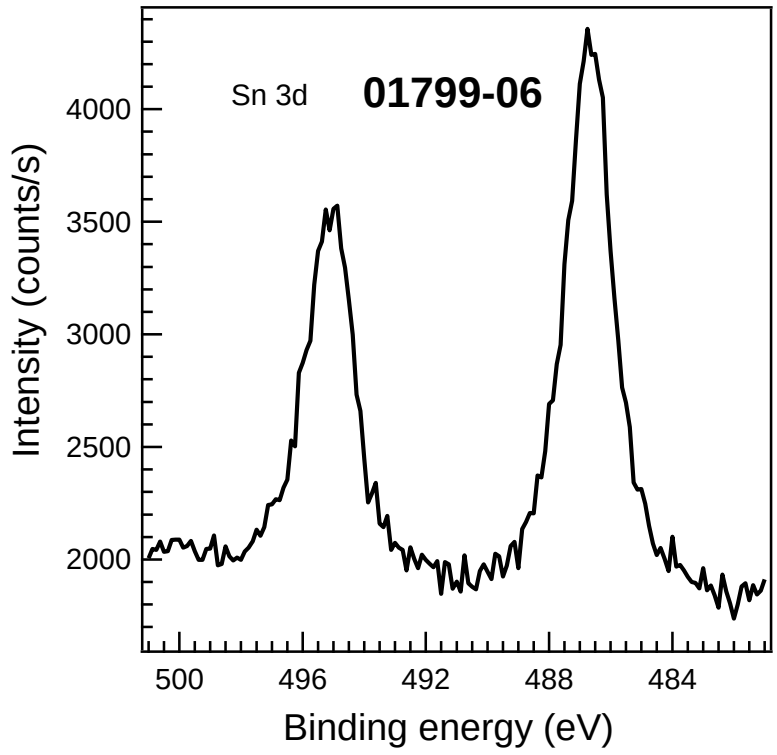

Publish in *SSS*: Yes X No ☐

- **Accession #: 01799-06**
- **Host Material:** C_3N_4-Au
- **Technique:** XPS
- **Spectral Region:** Sn 3d

Instrument: Perkin-Elmer Physical Electronics, Inc. 5600ci
Excitation Source: Al Ka
Source Energy: 1486.6 eV
Source Strength: 200 W
Source Size: >25 mm x >25 mm
Analyzer Type: spherical sector
Incident Angle: 9 °
Emission Angle: 45 °
Analyzer Pass Energy 58.7 eV
Analyzer Resolution: 0.6 eV
Total Signal Accumulation Time: 209.0 s
Total Elapsed Time: 229.9 s
Number of Scans: 20
Effective Detector Width: 0.6 eV

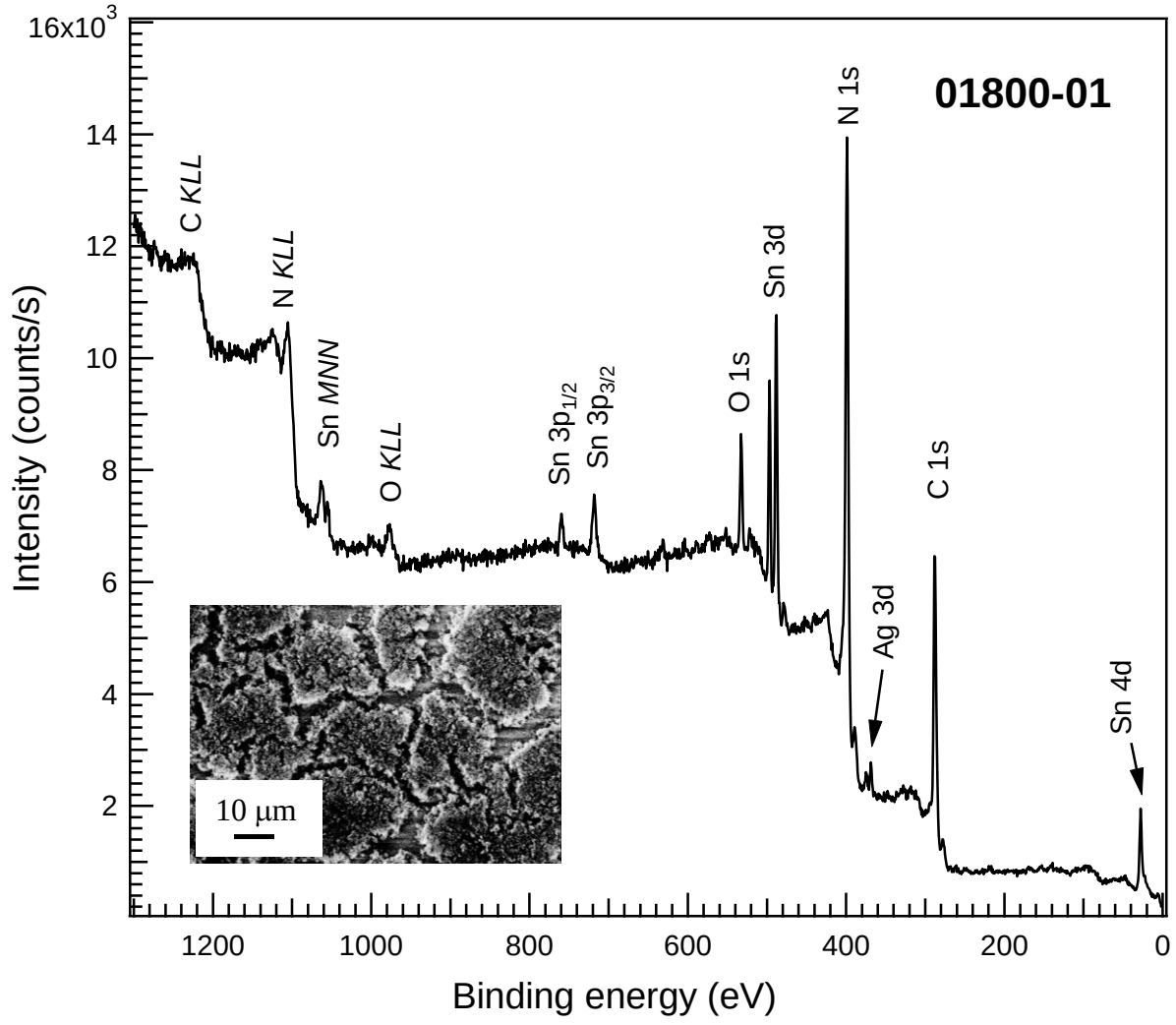

Publish in *Surface Science Spectra*: Yes ☒ No ☐

Accession #	01800-01
Host Material	C_3N_4-Ag
Technique	XPS
Spectral Region	survey
Instrument	Perkin-Elmer Physical Electronics, Inc. 5600ci
Excitation Source	Al Ka
Source Energy	1486.6 eV
Source Strength	200 W
Source Size	>25 mm x >25 mm
Analyzer Type	spherical sector analyzer
Incident Angle	9 ˚
Emission Angle	45 ˚
Analyzer Pass Energy	187.85 eV
Analyzer Resolution	1.9 eV
Total Signal Accumulation Time	1691.0 s
Total Elapsed Time	1860.1 s
Number of Scans	52
Effective Detector Width	1.9 eV

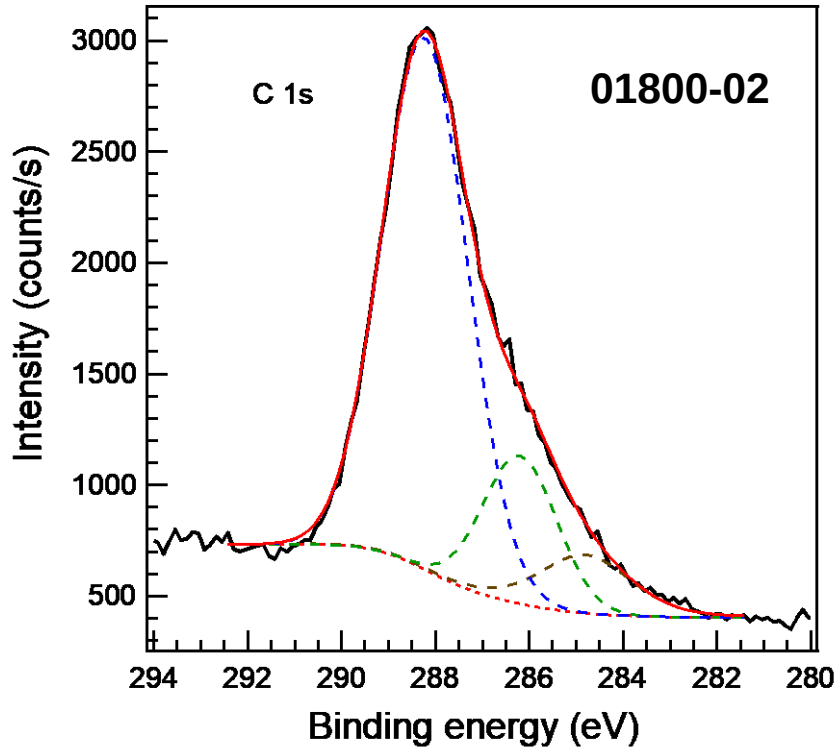

Publish in *SSS*: Yes X No ☐

- **Accession #: 01800-02**
- **Host Material:** C_3N_4-Ag
- **Technique:** XPS
- **Spectral Region:** C 1s

Instrument: Perkin-Elmer Physical Electronics, Inc. 5600ci
Excitation Source: Al Ka
Source Energy: 1486.6 eV
Source Strength: 200 W
Source Size: >25 mm x >25 mm
Analyzer Type: spherical sector
Incident Angle: 9 °
Emission Angle: 45 °
Analyzer Pass Energy 58.7 eV
Analyzer Resolution: 0.6 eV
Total Signal Accumulation Time: 277.5 s
Total Elapsed Time: 305.3 s

Number of Scans: 30

Effective Detector Width: 0.6 eV

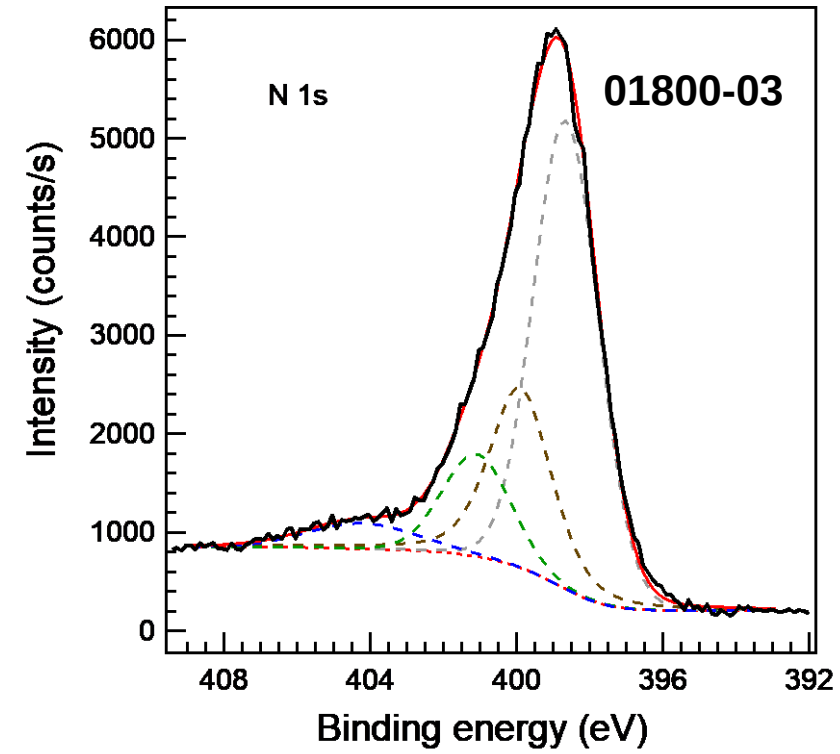

Publish in *SSS*: Yes X No ☐

- **Accession #: 01800-03**
- **Host Material:** C_3N_4-Ag
- **Technique:** XPS
- **Spectral Region:** N 1s

Instrument: Perkin-Elmer Physical Electronics, Inc. 5600ci
Excitation Source: Al Ka
Source Energy: 1486.6 eV
Source Strength: 200 W
Source Size: >25 mm x >25 mm
Analyzer Type: spherical sector
Incident Angle: 9 °
Emission Angle: 45 °
Analyzer Pass Energy 58.7 eV
Analyzer Resolution: 0.6 eV
Total Signal Accumulation Time: 301.5 s
Total Elapsed Time: 331.7 s

Number of Scans: 30

Effective Detector Width: 0.6 eV

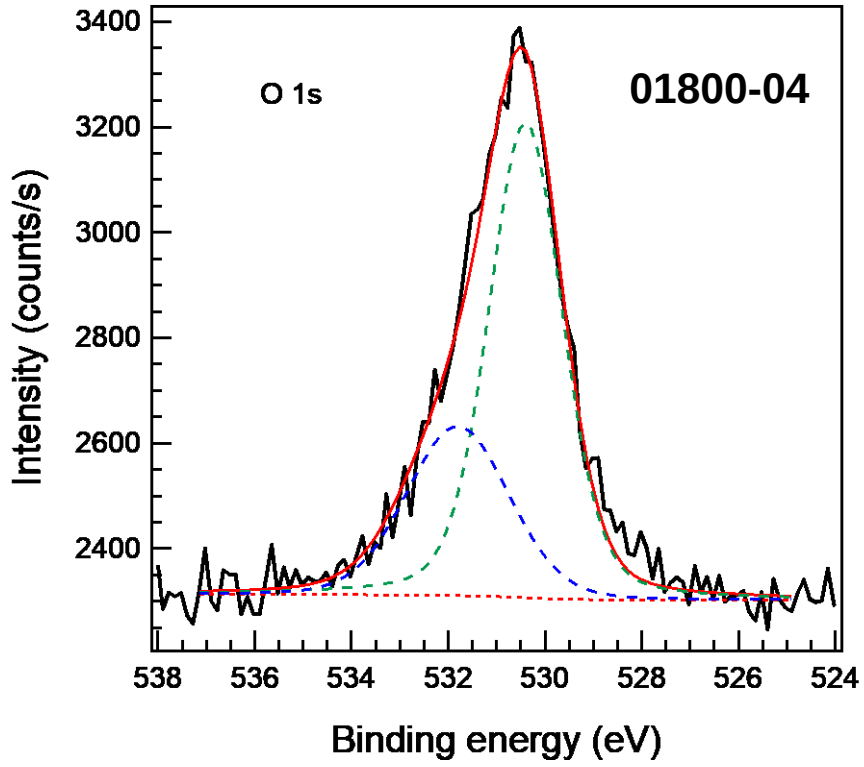

Publish in *SSS*: Yes ☒ No ☐

- **Accession #: 01800-04**
- **Host Material:** C_3N_4-Ag
- **Technique:** XPS
- **Spectral Region:** O 1s

Instrument: Perkin-Elmer Physical Electronics, Inc. 5600ci
Excitation Source: Al Ka
Source Energy: 1486.6 eV
Source Strength: 200 W
Source Size: >25 mm x >25 mm
Analyzer Type: spherical sector
Incident Angle: 9 °
Emission Angle: 45 °
Analyzer Pass Energy 58.7 eV
Analyzer Resolution: 0.6 eV
Total Signal Accumulation Time: 322.0 s
Total Elapsed Time: 354.2 s

Number of Scans: 40

Effective Detector Width: 0.6 eV

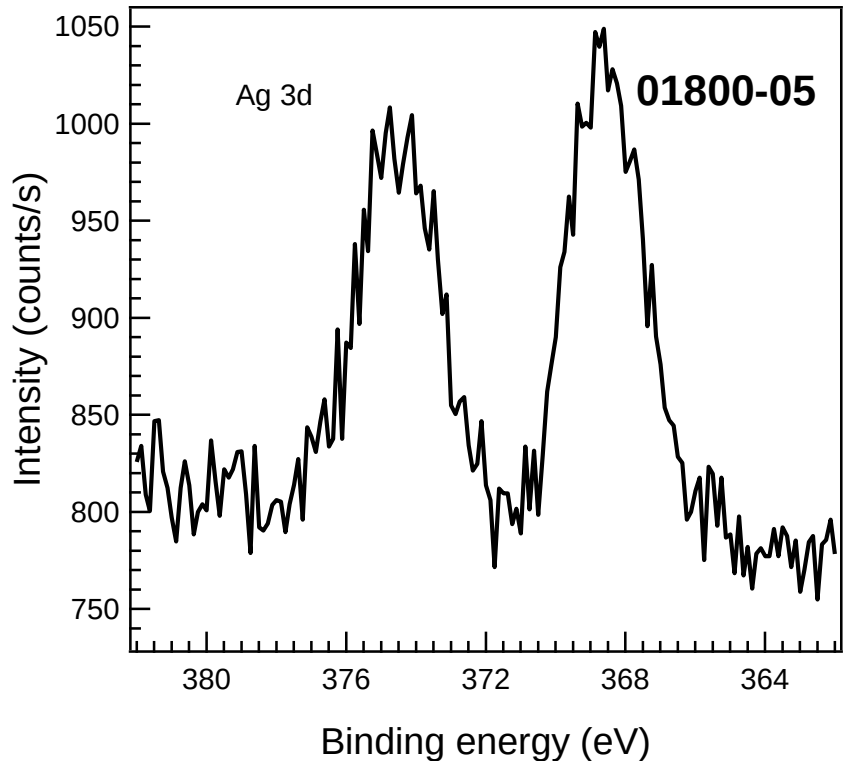

Publish in *SSS*: Yes ☒ No ☐

- **Accession #: 01800-05**
- **Host Material:** C_3N_4-Ag
- **Technique:** XPS
- **Spectral Region:** Ag 3d

Instrument: Perkin-Elmer Physical Electronics, Inc. 5600ci
Excitation Source: Al Ka
Source Energy: 1486.6 eV
Source Strength: 200 W
Source Size: >25 mm x >25 mm
Analyzer Type: spherical sector
Incident Angle: 9 °
Emission Angle: 45 °
Analyzer Pass Energy 58.7 eV
Analyzer Resolution: 0.6 eV
Total Signal Accumulation Time: 522.5 s
Total Elapsed Time: 574.8 s

Number of Scans: 50

Effective Detector Width: 0.6 eV

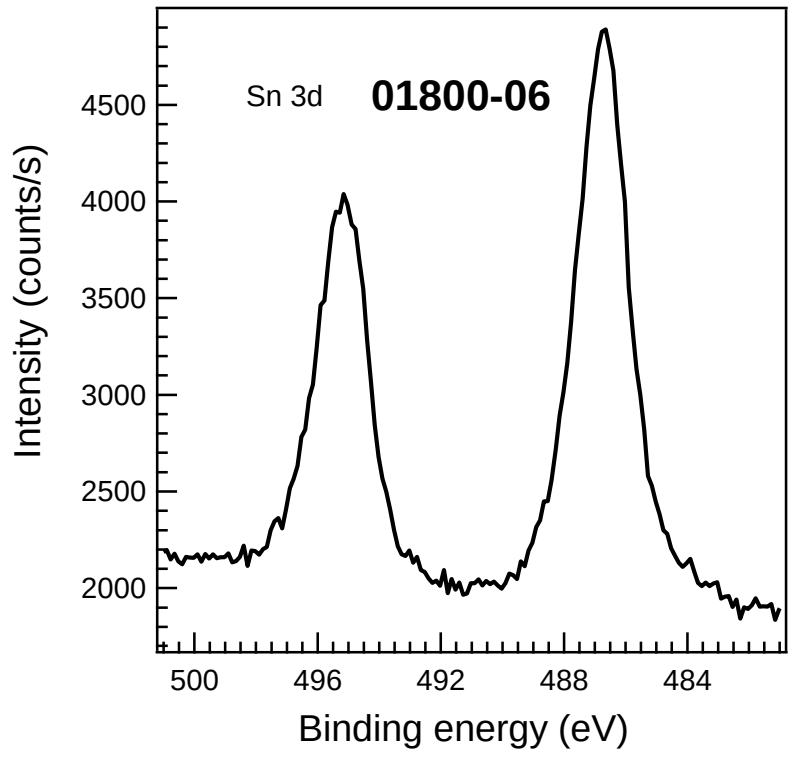

Publish in *SSS*: Yes X No ☐

- **Accession #: 01800-06**
- **Host Material:** C_3N_4-Ag
- **Technique:** XPS
- **Spectral Region:** Sn 3d

Instrument: Perkin-Elmer Physical Electronics, Inc. 5600ci
Excitation Source: Al Ka
Source Energy: 1486.6 eV
Source Strength: 200 W
Source Size: >25 mm x >25 mm
Analyzer Type: spherical sector
Incident Angle: 9 °
Emission Angle: 45 °
Analyzer Pass Energy 58.7 eV
Analyzer Resolution: 0.6 eV
Total Signal Accumulation Time: 418.0 s
Total Elapsed Time: 459.8 s
Number of Scans: 40
Effective Detector Width: 0.6 eV

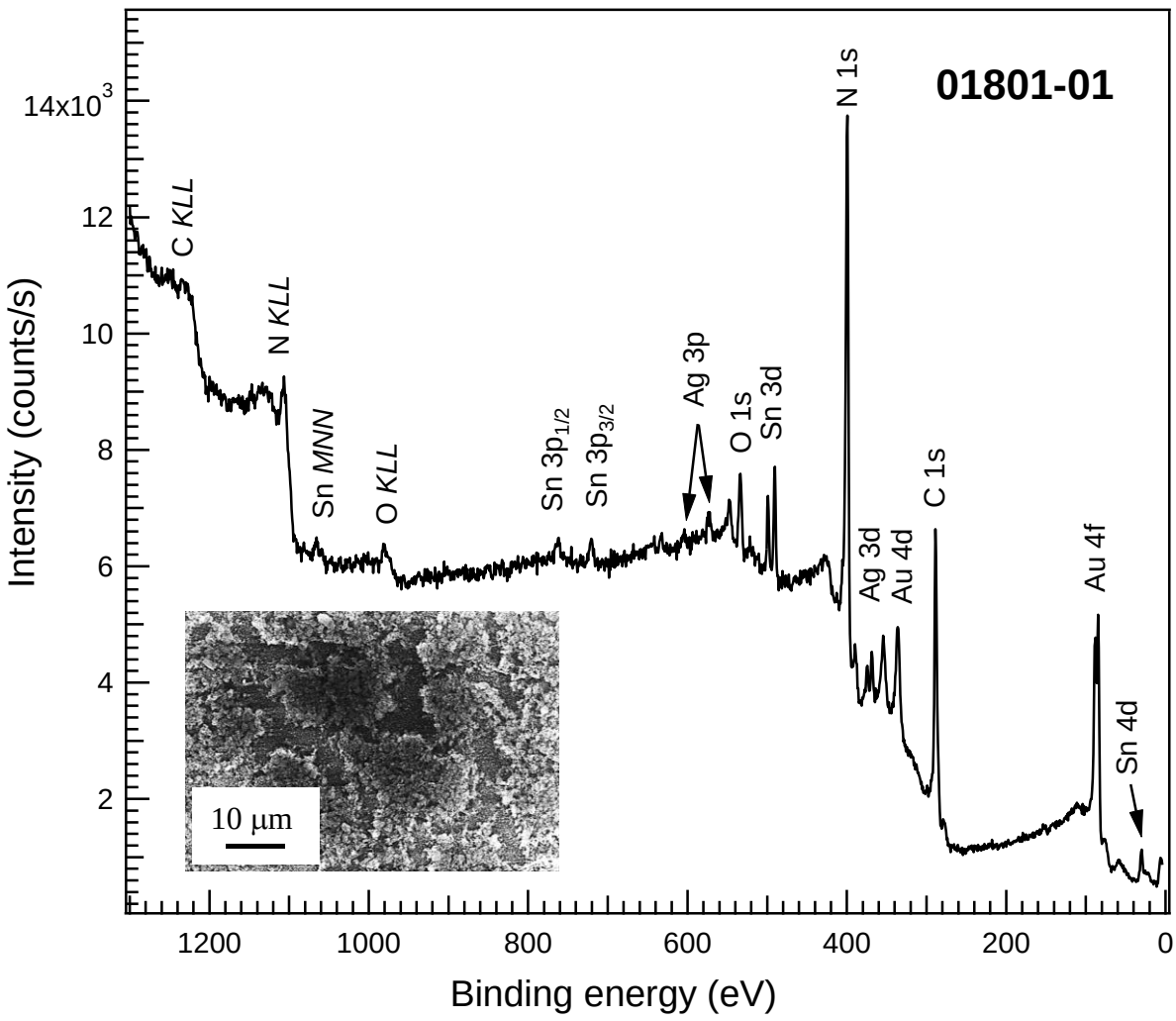

Publish in *Surface Science Spectra*: Yes X No ☐

Accession #	01801-01
Host Material	C_3N_4-Au-Ag
Technique	XPS
Spectral Region	survey
Instrument	Perkin-Elmer Physical Electronics, Inc. 5600ci
Excitation Source	Al Ka
Source Energy	1486.6 eV
Source Strength	200 W
Source Size	>25 mm x >25 mm
Analyzer Type	spherical sector analyzer
Incident Angle	9 ˚
Emission Angle	45 ˚
Analyzer Pass Energy	187.85 eV
Analyzer Resolution	1.9 eV
Total Signal Accumulation Time	1626.0 s
Total Elapsed Time	1788.6 s
Number of Scans	50
Effective Detector Width	1.9 eV

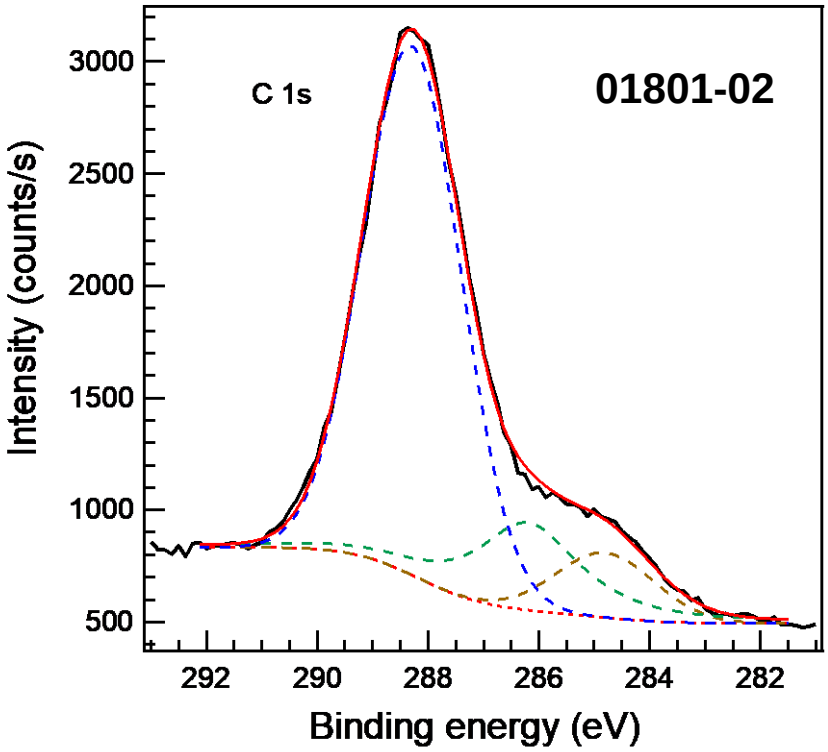

Publish in *SSS*: Yes X No ☐

- **Accession #: 01801-02**
- **Host Material:** C_3N_4-Au-Ag
- **Technique:** XPS
- **Spectral Region:** C 1s

Instrument: Perkin-Elmer Physical Electronics, Inc. 5600ci
Excitation Source: Al Ka
Source Energy: 1486.6 eV
Source Strength: 200 W
Source Size: >25 mm x >25 mm
Analyzer Type: spherical sector
Incident Angle: 9 °
Emission Angle: 45 °
Analyzer Pass Energy 58.7 eV
Analyzer Resolution: 0.6 eV
Total Signal Accumulation Time: 444.0 s
Total Elapsed Time: 488.4 s

Number of Scans: 48

Effective Detector Width: 0.6 eV

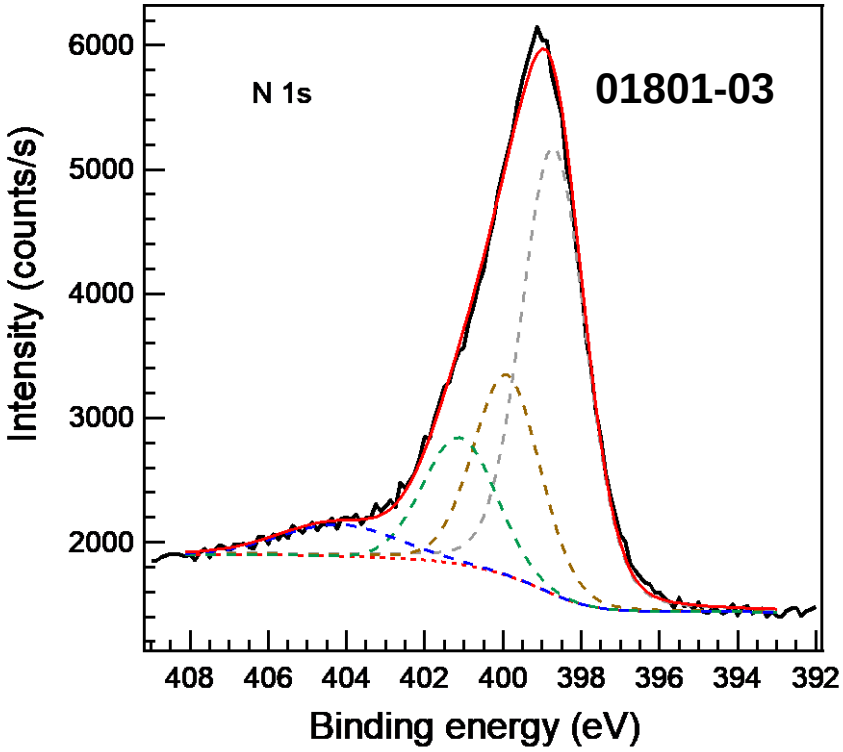

Publish in *SSS*: Yes X No ☐

- **Accession #: 01801-03**
- **Host Material:** C_3N_4-Au-Ag
- **Technique:** XPS
- **Spectral Region:** N 1s

Instrument: Perkin-Elmer Physical Electronics, Inc. 5600ci
Excitation Source: Al Ka
Source Energy: 1486.6 eV
Source Strength: 200 W
Source Size: >25 mm x >25 mm
Analyzer Type: spherical sector
Incident Angle: 9 °
Emission Angle: 45 °
Analyzer Pass Energy 58.7 eV
Analyzer Resolution: 0.6 eV
Total Signal Accumulation Time: 422.1 s
Total Elapsed Time: 464.3 s

Number of Scans: 42

Effective Detector Width: 0.6 eV

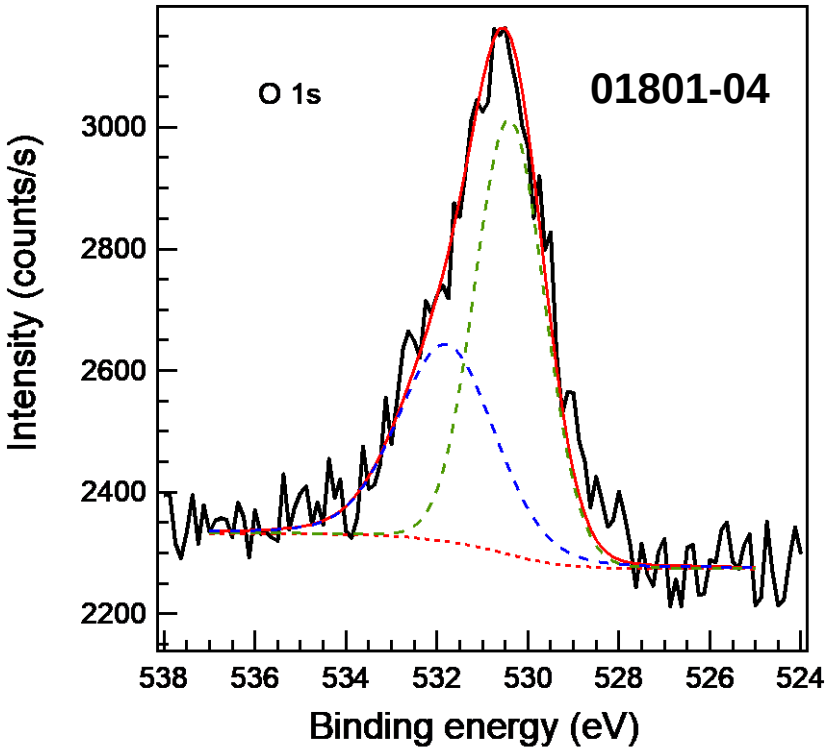

Publish in *SSS*: Yes ☒ No ☐

- **Accession #: 01801-04**
- **Host Material:** C_3N_4-Au-Ag
- **Technique:** XPS
- **Spectral Region:** O 1s

Instrument: Perkin-Elmer Physical Electronics, Inc. 5600ci
Excitation Source: Al Ka
Source Energy: 1486.6 eV
Source Strength: 200 W
Source Size: >25 mm x >25 mm
Analyzer Type: spherical sector
Incident Angle: 9 °
Emission Angle: 45 °
Analyzer Pass Energy 58.7 eV
Analyzer Resolution: 0.6 eV
Total Signal Accumulation Time: 161.0 s
Total Elapsed Time: 177.1 s

Number of Scans: 20

Effective Detector Width: 0.6 eV

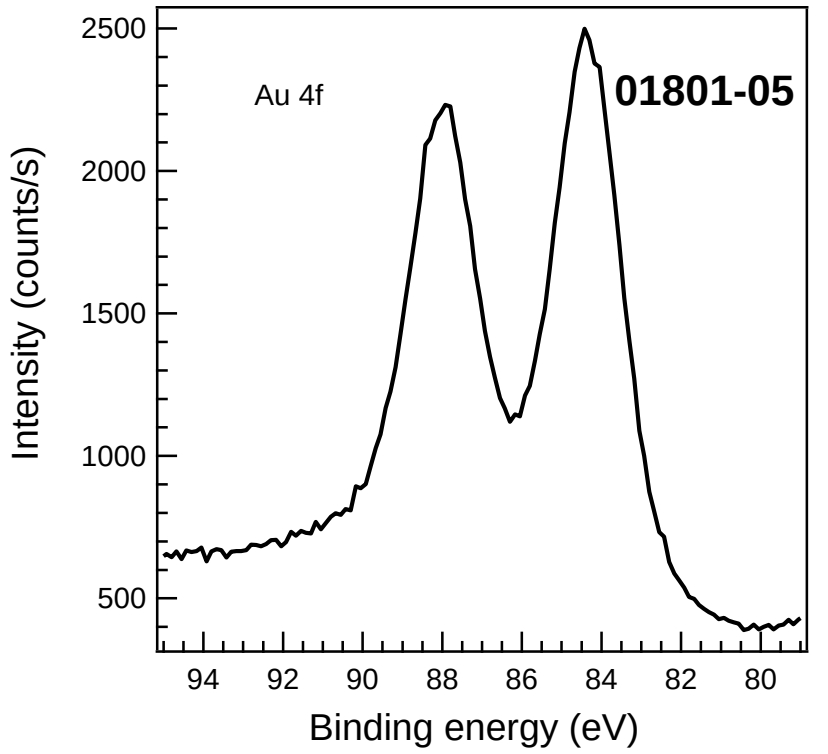

Publish in *SSS*: Yes ☒ No ☐

- **Accession #: 01801-05**
- **Host Material:** C_3N_4-Au-Ag
- **Technique:** XPS
- **Spectral Region:** Au 4f

Instrument: Perkin-Elmer Physical Electronics, Inc. 5600ci
Excitation Source: Al Ka
Source Energy: 1486.6 eV
Source Strength: 200 W
Source Size: >25 mm x >25 mm
Analyzer Type: spherical sector
Incident Angle: 9 °
Emission Angle: 45 °
Analyzer Pass Energy 58.7 eV
Analyzer Resolution: 0.6 eV
Total Signal Accumulation Time: 796.5 s
Total Elapsed Time: 876.2 s

Number of Scans: 90

Effective Detector Width: 0.6 eV

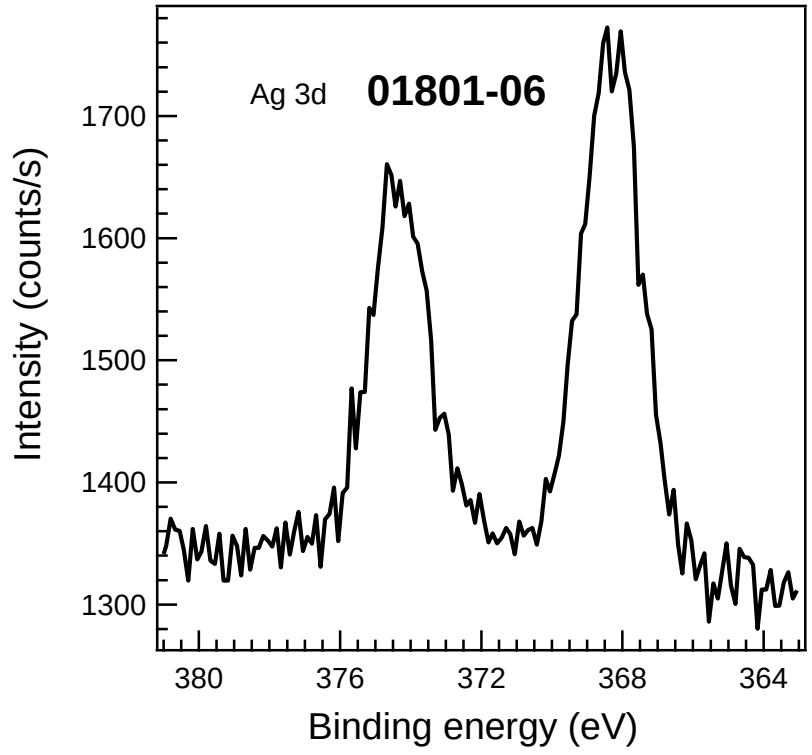

Publish in *SSS*: Yes ☒ No ☐

- **Accession #: 01801-06**
- **Host Material:** C_3N_4-Au-Ag
- **Technique:** XPS
- **Spectral Region:** Ag 3d

Instrument: Perkin-Elmer Physical Electronics, Inc. 5600ci
Excitation Source: Al Ka
Source Energy: 1486.6 eV
Source Strength: 200 W
Source Size: >25 mm x >25 mm
Analyzer Type: spherical sector
Incident Angle: 9 °
Emission Angle: 45 °
Analyzer Pass Energy 58.7 eV
Analyzer Resolution: 0.6 eV
Total Signal Accumulation Time: 1206.0 s
Total Elapsed Time: 1326.6 s

Number of Scans: 120

Effective Detector Width: 0.6 eV

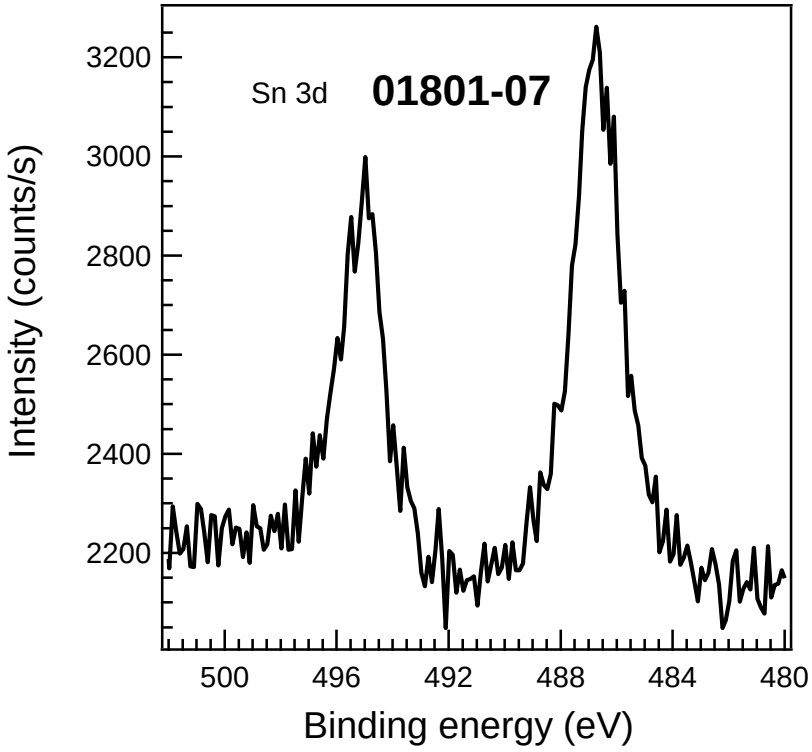

Publish in *SSS*: Yes ☒ No ☐

- **Accession #: 01801-07**
- **Host Material:** C_3N_4-Au-Ag
- **Technique:** XPS
- **Spectral Region:** Sn 3d

Instrument: Perkin-Elmer Physical Electronics, Inc. 5600ci
Excitation Source: Al Ka
Source Energy: 1486.6 eV
Source Strength: 200 W
Source Size: >25 mm x >25 mm
Analyzer Type: spherical sector
Incident Angle: 9 °
Emission Angle: 45 °
Analyzer Pass Energy 58.7 eV
Analyzer Resolution: 0.6 eV
Total Signal Accumulation Time: 209.0 s
Total Elapsed Time: 229.9 s

Number of Scans: 20

Effective Detector Width: 0.6 eV